

# LOAD CAPACITY OF ANCHORAGES IN SOLID CALCIUM SILICATE MASONRY WITH BRICK BREAKOUT FAILURE

## DAS TRAGVERHALTEN VON VERANKERUNGEN IN KALKSANDVOLLSTEINEN BEI STEINAUSBRUCH

Mehdiye Panzehir, Jan Hofmann

*Institute of Construction Materials (IWB), University of Stuttgart*

### SUMMARY

The aim of this paper is to determine the load-bearing behaviour of bonded anchors in solid calcium silicate bricks in case of brick breakout failure under tension loading. For this purpose, experimental tests with bonded anchors and undercut anchors were carried out at the Institute of Construction Materials (IWB) of the University of Stuttgart. Solid calcium silicate bricks with different dimensions and compressive strengths were used as base material.

This paper investigates if the fracture mechanism in solid calcium silicate brick in case of breakout failure is comparable with the behaviour in concrete. Tests have shown the influence of the embedment depth with an exponent of 1.5 ( $h_{ef}^{1.5}$ ) as in concrete.

### ZUSAMMENFASSUNG

Gegenstand dieser Arbeit ist es, das Tragverhalten von Verbunddübel in Kalksandvollsteinen bei der Versagensart Steinausbruch unter zentrischer Zugbelastung zu ermitteln. Zu diesem Zweck wurden experimentelle Untersuchungen mit Verbunddübel und Hinterschnittanker am Institut für Werkstoffe im Bauwesen (IWB) der Universität Stuttgart durchgeführt. Als Ankergrund dienten Kalksandvollsteine mit verschiedenen Formaten und Druckfestigkeiten.

Es soll untersucht werden, ob der Bruchmechanismus in Kalksandvollstein im Falle eines Ausbruchsversagens mit dem Verhalten in Beton vergleichbar ist. Bei Versuchen konnte der Einfluss der Verankerungstiefe mit einem Exponenten von 1,5 ( $h_{ef}^{1,5}$ ) wie in Beton aufgezeigt werden.

## 1. INTRODUCTION

For centuries, one of the most popular construction materials has been masonry. Meanwhile, newly developed materials have been used to meet further requirements such as thermal insulation, sound proofing, fire protection, etc.

Since masonry walls are increasingly present in both old and new buildings, research has been conducted in this area and design models for bonded anchors and plastic anchors have been established [1, 2, 3, 4, 5]. Even though research in this direction has been carried out, the state of the art of the load-bearing behaviour for bonded anchors in masonry is not as extensive as for concrete. Therefore, further experimental tests were carried out to complement the present design model.

In the current design model Technical Report 054 (TR054) [6], equations for calculating the resistance for tension and shear loads are not available for all failure modes, as for bonded anchors in concrete, see TR029 [7]. For the characteristic resistance to tension load equations for the failure modes steel failure, brick pull-out and combined failure are available. There is no equation for the characteristic resistance in case of pull-out failure of the anchor or brick breakout failure. For these failure modes, reference is made to the respective European Technical Assessment (ETA). There is also no equation to determine the characteristic resistance to shear loading for all failure modes. There are only equations for steel failure, brick edge failure and pushing out of one brick. For the failure mode local brick failure, reference is made to the respective value in the ETA.

In this paper the results of investigations on the brick breakout failure mode under tension loading is presented. Furthermore, an existing design model [1] is compared with the test results and a proposal for an improved model for the brick breakout failure of solid calcium silicate bricks is made.

## 2. EXPERIMENTAL PROGRAMME

The tests with bonded anchors (BA) were carried out with bricks of various dimensions. Bonded anchors with and without sieve sleeves were investigated. The injection mortar consists of two components that are stored in a 2-chamber cartridge. The two components combine and react when dispensed through a static mixing nozzle. In all tests, threaded rods of size M8 or M12 with a steel grade of 8.8 were used. Plastic sieve sleeves had a diameter of 12 mm. The embedment

depth was for all tests 50 mm. Solid calcium silicate bricks in the dimensions 8 DF and plan elements (PE) with a compressive strength class of 12 N/mm<sup>2</sup> and 16 N/mm<sup>2</sup> and a bulk density class of 2.0 kg/dm<sup>3</sup> were used as base material. The nominal compressive strengths of the bricks were determined according to DIN EN 772-1 at the Materials Testing Institute (MPA) of the University of Stuttgart. They were for the 8 DF bricks 15.2 N/mm<sup>2</sup> and for PE blocks 18.1 N/mm<sup>2</sup> for the dimension 998 x 300 x 498 mm and 21.2 N/mm<sup>2</sup> for the dimension 998 x 300 x 623 mm [8]. Tests were carried out in single masonry units.

The tests with undercut anchors (UA) were carried out with various embedment depths  $h_{ef}$  in PE. The mechanical anchor is a self-cutting undercut anchor made of galvanized steel. In the tests, anchors of size M10 and M16 were used. Solid calcium silicate bricks in two dimensions of PE with a compressive strength class of 16 N/mm<sup>2</sup> and a bulk density class of 2.0 kg/dm<sup>3</sup> were used as base material. The nominal compressive strengths of the bricks were determined according to DIN EN 772-1 at the MPA of the University of Stuttgart and was 18.1 N/mm<sup>2</sup> for the dimension 998 x 300 x 498 mm and 21.2 N/mm<sup>2</sup> for the dimension 998 x 300 x 623 mm [8]. To obtain a complete breakout unaffected by edges, the tests were only carried out in single PE blocks.

A summary of the performed tests is listed in Table 1. If the masonry unit failed due to splitting, no further tests were carried out, so the number of tests in various series is different.

Table 1: Test programme

Series	No. of tests	Anchor System	Embedment Depth $h_{ef}$	Brick Dimension	Support width
BA-M8	10	BA M8	50 mm	8 DF / PE	250 mm
BA-M8-s	5	BA M8-s	50 mm	8DF	250 mm
BA-M12	6	BA M12	50 mm	PE	440 mm
UA- $h_{ef}$ 40	5	UA M10	40 mm	PE	440 mm
UA- $h_{ef}$ 50	5	UA M10	50 mm	PE	440 mm
UA- $h_{ef}$ 60	5	UA M10	60 mm	PE	440 mm
UA- $h_{ef}$ 70	5 / 2	UA M10/ M16	70 mm	PE	440 mm
UA- $h_{ef}$ 90	5	UA M10	90 mm	PE	440 mm
UA- $h_{ef}$ 100	5	UA M10	100 mm	PE	440 mm
UA- $h_{ef}$ 110	1 / 3	UA M10/ M16	110 mm	PE	440 mm
UA- $h_{ef}$ 120	4	UA M16	120 mm	PE	440 mm
UA- $h_{ef}$ 130	2	UA M16	130 mm	PE	440 mm
UA- $h_{ef}$ 140	1	UA M16	140 mm	PE	440 mm
UA- $h_{ef}$ 150	1	UA M16	150 mm	PE	440 mm
UA- $h_{ef}$ 190	2	UA M16	190 mm	PE	440 mm

## 2.1 Installation Procedure

For test series of bonded anchors (BA) with threaded rods size M8, the holes were drilled using a rotary hammer with a drilling rig and hardened metal drill bit with the required cutting diameter ( $d_{cut}$ ) of 12 mm. The drilling rig was used to ensure that the drill holes are perpendicular to the surface. After drilling, the cleaning was done according to the manufacturer's printed installation instructions (MPII). Next, sieve sleeves were inserted into the hole for tests with sieve sleeve, after that the mortar was injected directly into the sieve sleeve and then the threaded rods were inserted. For tests without sieve sleeve, after cleaning procedure the mortar was injected directly into the hole and then the threaded rods were inserted. The tests were performed after the minimum curing time of the mortar.

For test series of bonded anchors (BA) with threaded rods size M12, the holes are drilled using a rotary hammer with a drilling rig and hardened metal drill bit with the required cutting diameter ( $d_{cut}$ ) of 14 mm. The next steps are as described as for bonded anchors with threaded rods size M8 without inserting a sieve sleeve.

For test series of undercut anchors (UA), the holes are drilled through the loading fixture using a rotary hammer with a drilling rig and hardened metal drill bit with the required cutting diameter ( $d_{cut}$ ) of 20 mm for size M10 and 30 mm for size M16. After drilling, the cleaning was done according to the manufacturer's printed installation instructions (MPII). Afterwards, the anchor was inserted into the hole, with the help of a setting tool, and the expansion elements formed an undercut into the calcium silicate brick.

## 2.2 Experimental Procedure

For two test series on bonded anchors 8DF solid bricks served as base material whereas Plane Element block have been used for tests on bonded anchors and undercut anchors (Table 1). The bonded anchor was tested with an effective embedment depth of 50 mm, which could also be installed in small format bricks without edge influence. However, as the brick failed in some tests due to splitting, further tests were carried out in PE blocks to obtain a complete brick breakout failure. All tests were carried out in single masonry unit. The bricks, the embedment depths and the corresponding support diameters are given in Table 1. All tests were loaded axially by means of a hydraulic cylinder. The load was transferred from the cylinder with an attachment part via a threaded rod. The vertical anchor displacement was transferred from the anchor top to a linear

voltage displacement transducer (LVDT) by means of a wire. Fig. 1 illustrates the applied test setups, in which a support width of  $4 h_{ef}$  was maintained.



*Fig. 1: Unconfined test setup for tests with bonded anchors (left) and with undercut anchors (right) [9]*

### 3. TEST RESULTS

#### 3.1 Tests at the IWB

A total of 14 test series with 67 tests were carried out, whereby only tests with brick breakout failure were evaluated. Table 2 summarizes all brick breakout failure results (49 tests). The first column of Table 2 describes the series with the letters BA or UA for the anchor systems bonded anchor or undercut anchor, respectively. The following number of BA shows the anchor size and finally s is used in case of installation with sieve sleeve. The following positions for UA indicate the size and then the embedment depth of the anchor. In the other columns the brick dimensions, the ultimate load ( $N_u$ ) in series with one test without the standard deviation or the mean ultimate load ( $N_{u,m}$ ) and the standard deviation of tests are listed.

In the tests, brick breakout failure occurred in approx. 75 % of cases, 16 % of the tests failed by splitting and 8 % failed by pull-out or combined failure. Fig. 2 shows brick breakout failure of bonded anchors and undercut anchors. The shape of brick breakout is similar to the concrete cone failure. It is also cone-shaped and

the angle between the cone and the stone surface of the brick is approximately 35°.

Table 2: Test results

Series	No. of tests	Brick Dimension	$N_u$ or $N_{u,m}$ [kN]	Standard deviation [%]
BA-M8	3	8DF	12.17	2.3
BA-M8	2	PE	12.65	13.0
BA-M8-s	1	8 DF	9.91	-
BA-M12	6	PE	12.02	11.9
UA-M10- $h_{ef}$ 40	5	PE	10.35	6.1
UA-M10- $h_{ef}$ 50	5	PE	14.00	13.9
UA-M10- $h_{ef}$ 60	5	PE	18.46	10.2
UA-M10- $h_{ef}$ 70	5	PE	21.24	10.2
UA-M16- $h_{ef}$ 70	2	PE	29.42	5.6
UA-M10- $h_{ef}$ 90	5	PE	29.39	5.3
UA-M10- $h_{ef}$ 100	5	PE	32.62	1.8
UA-M10- $h_{ef}$ 110	1	PE	38.33	-
UA-M16- $h_{ef}$ 110	2	PE	47.71	2.0
UA-M16- $h_{ef}$ 120	2	PE	54.32	



Fig. 2: Brick breakout failure with bonded anchor (left) and undercut anchor (right) [9]

### 3.2 Tests at the MPA

In order to check the material properties, 3-point bending tests were carried out on solid calcium silicate bricks at the MPA of the University of Stuttgart. Four different thicknesses of beams have been tested. The sizes of the bending beams were doubled. Only the last size was enlarged by a factor of 1.5, as it was not possible to produce the larger test specimens with the plane element block. The thicknesses and widths of the beams were 20 mm, 40 mm, 80 mm and 120 mm. Furthermore, the span lengths were 50 mm, 100 mm, 200 mm and 300 mm. The respective test beams were sawn from plane element blocks so that all test specimens come from one batch and the results are only influenced by the specimen sizes. The tests were carried out in accordance with DIN EN 772-6 [10].

A schematic drawing of the test procedure is shown in Fig. 3. The beams did not have a notch on the underside. During the test, the beams were placed on two roller supports with the required span length. Another roller with the same diameter as the lower rollers, located in the centre of the beam is used to apply the load from above. For this, the load is applied continuously and without impact until failure.

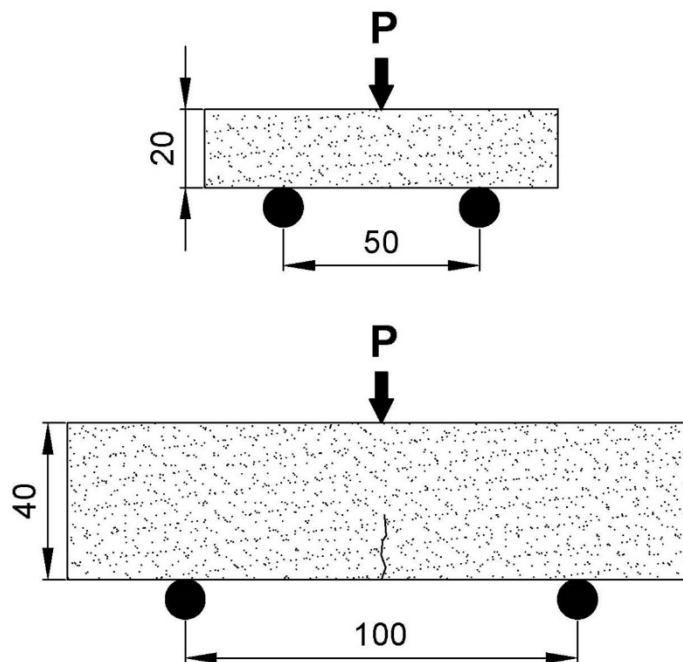


Fig. 3: Schematic drawing of the 3-point bending tests, in mm [9]

## 4. DISCUSSION

### 4.1 Three-point Bending Tests

It was the aim to investigate the size effect in detail and to get information about the influence of the failure mode brick breakout. Fig. 4 illustrates the ultimate loads  $N_u$  of the 3-point bending tests vs. beam thickness. The test results show an increase in ultimate load with increasing of the beam thickness. When the beam thickness and support width are doubled, the increase in ultimate loads is significant. The increase is a function of the beam depth to the power of 1.5. With the non-linear regression, the coefficient of determination is 0.98. These results indicate that the influence of the embedment depth regarding brick failure loads will also increase with the embedment depth with a power of 1.5 ( $h_{ef}^{1.5}$ ). This assumption needs to be confirmed.

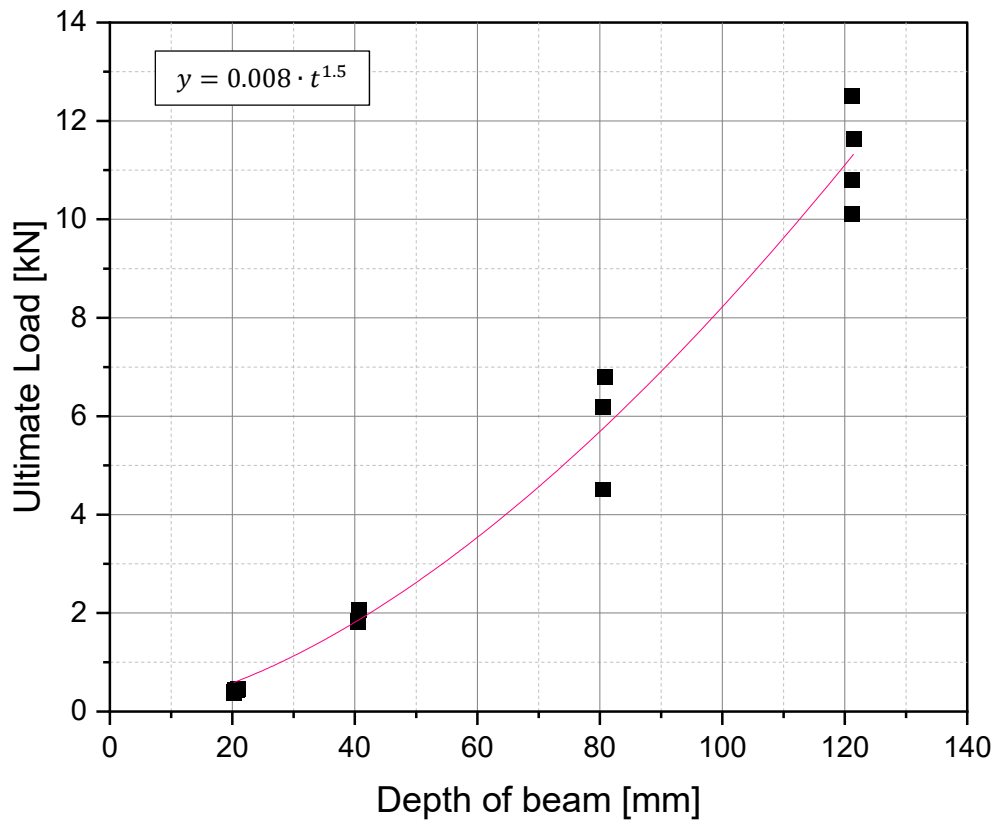


Fig. 4: Ultimate load  $N_u$  vs. depth of the beam [9]

#### 4.2 Influence of the Compressive Strength

The influence of brick compressive strength  $f_b$  on the load-bearing behaviour in case of brick breakout failure can be determined using data from Meyer (2006) [1]. A total of 93 tests with the failure mode brick breakout and with an unconfined test setup were evaluated in the following. The tests listed in Section 3 include tests with undercut anchors, because the behaviour of the base material is crucial, and the anchorage system seems to be secondary.

The results are plotted as related values against the compressive strength  $f_b$  in Fig. 5. In order to determine the influence of the compressive strength  $f_b$ , the ultimate loads were divided by the embedment depth  $h_{ef}$  to the power of 1.5, based on the behaviour of the three-point bending tests described in Section 4.1. Black squares represent the results with bonded anchors. Red squares represent the results with undercut anchors and white squares represent the results with bonded anchors from Meyer (2006) [1]. The increase is dependent on the brick compressive strength  $f_b$  with a power of 0.3 ( $f_b^{0.3}$ ) according to the regression curve. With these tests, the range from 12.3 N/mm<sup>2</sup> to 21.2 N/mm<sup>2</sup> is considered. The compressive strength classes for calcium silicate bricks are standardized



between 4 N/mm<sup>2</sup> and 60 N/mm<sup>2</sup>, but in practice the compressive strength classes 12 N/mm<sup>2</sup> and 20 N/mm<sup>2</sup> mainly produced [11]. This means that the average compressive strengths are between 15 and 25 N/mm<sup>2</sup>. Thus, the specific influence of the compressive strength applies to the main area of application.

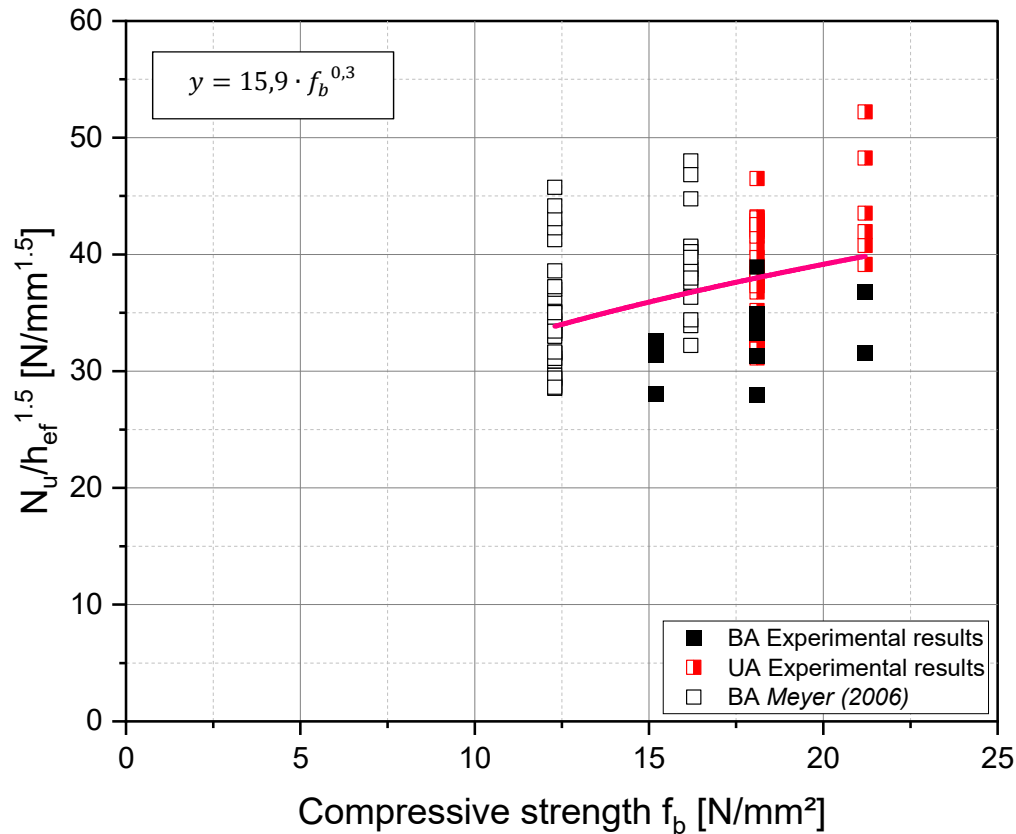


Fig. 5: Influence of compressive strength on brick breakout failure [9]

In order to be able to compare the test results with each other, the ultimate loads  $N_u$  must be normalized to a specific compressive strength. In EAD 330076, the normalized ultimate load  $N_{u,norm}$  is determined using following equation:

$$N_{u,norm} = N_u \cdot (f_{b,norm}/f_{b,test})^\alpha \quad (1)$$

With:

$f_{b,norm}$  Normalized compressive strength [N/mm<sup>2</sup>]

$f_{b,test}$  Compressive strength at the time of testing [N/mm<sup>2</sup>]

$\alpha$  = 0.5 for masonry units of clay or concrete and solid unit of calcium silicate [–]

This equation describes that the influence of the compressive strength  $f_b$  is included in the calculation with a power of 0.5. As described above, this value is

better represented by a value of 0.3. Therefore, in the following for the exponent in Eq. (1)  $\alpha = 0.3$  is used.

### 4.3 Influence of the Embedment Depth

Fig. 6 shows the normalized ultimate loads  $N_{u,norm}$  plotted against the embedment depth  $h_{ef}$  using Eq. (1) with  $\alpha = 0.3$ . Black squares represent the results with bonded anchors. Half squares represent the results with undercut anchors and white squares represent the results with bonded anchors from Meyer (2006) [1]. These results confirm that the ultimate load increases with a power of 1.5 as a function of the embedment depth. The coefficient of determination of the non-linear regression is 0.97.

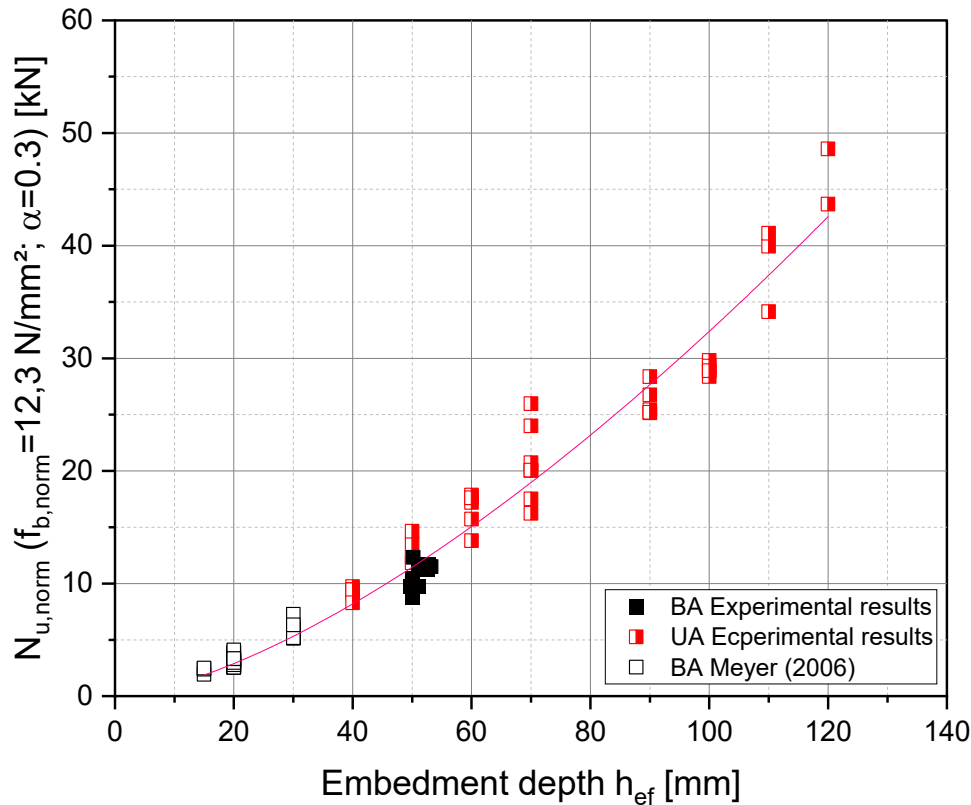


Fig. 6: Influence of embedment depth on brick breakout failure [9]

### 4.4 Integration of the Influences for Calculation of Ultimate Load

Based on the results of the investigations, the equation for calculating the failure load in case of brick breakout is derived. The pre-factor  $k_{CS} = 15.0$  was determined empirically from an assessment of a total number of 93 tests.

$$N_{u,b}^0 = k_{CS} \cdot f_b^{0.3} \cdot h_{ef}^{1.5} [N] \quad (2)$$

With:

$k_{CS}$  = 15.0 pre-factor [–]

$f_b$  Normalized mean brick compressive strength [ $N/mm^2$ ]

$h_{ef}$  Embedment depth [ $mm$ ]

A comparison of the results with the ultimate load at brick breakout failure to Eq. (2) is illustrated in Fig. 6. In addition, the results of Meyer (2006) [1] are included in the chart. As demonstrated in Fig. 7, the proposed equation is in good agreement with the experimental results.

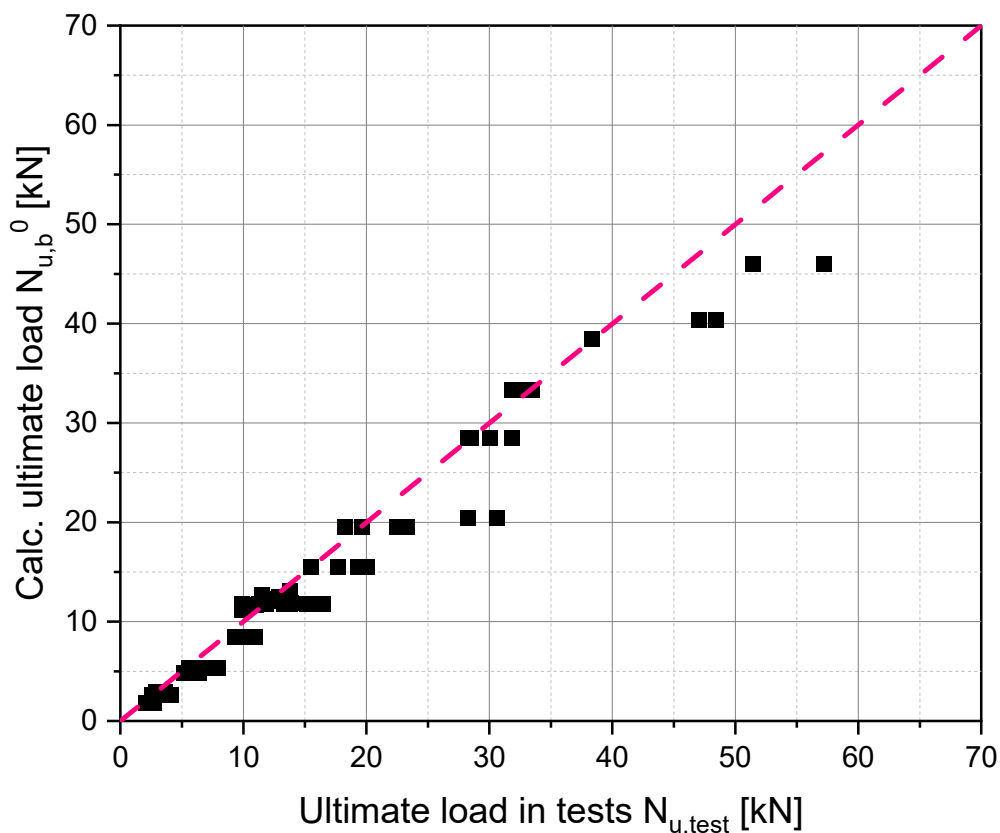


Fig. 7: Calculated loads acc. to Eq. (3) vs. ultimate loads at the tests [9]

Fig. 8 and Fig. 9 shows two diagrams, each representing the ratio of the calculated ultimate load  $N_{u,calc}$  to the ultimate load of the tests  $N_{u,test}$ . The first graph shows the ratio against embedment depth and the second graph against brick compressive strength. The comparison  $N_{u,calc}$  to  $N_{u,test}$  results in a mean value of 1.02 with a coefficient of variation of 13.2 %. Both diagrams show, the distribution of the results is around the horizontal line at 1.0 and the influences embedment depth and compressive strength are well reflected in Eq. (2).

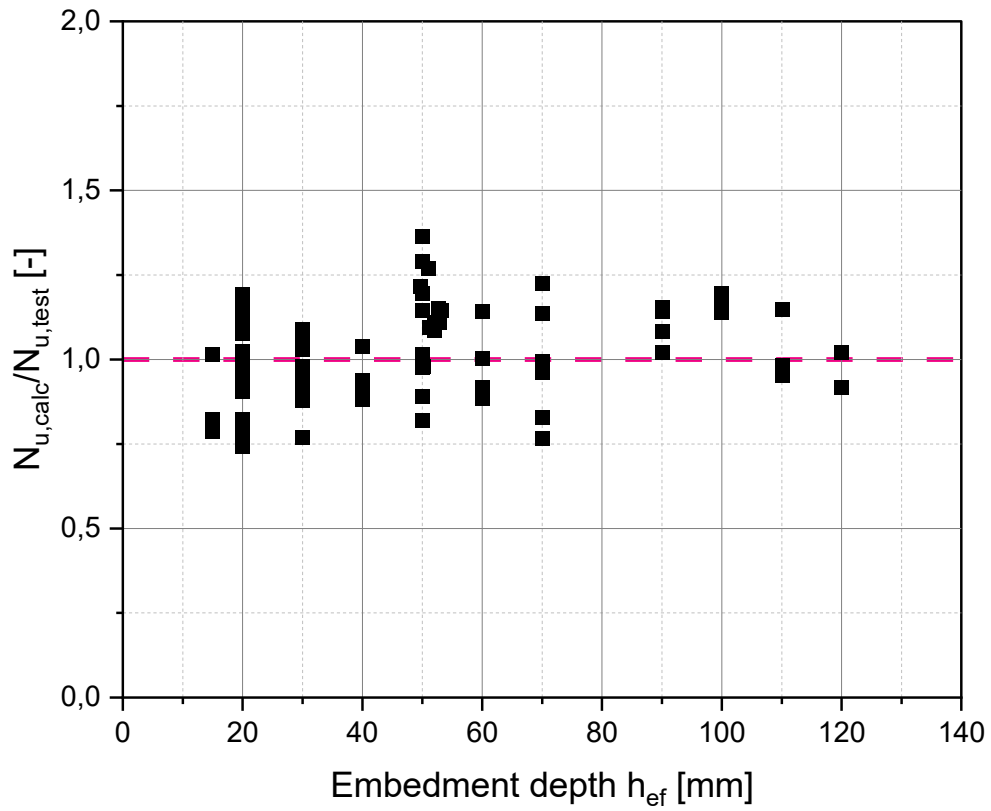


Fig. 8:  $N_{u,calc}/N_{u,test}$  vs. embedment depth [9]

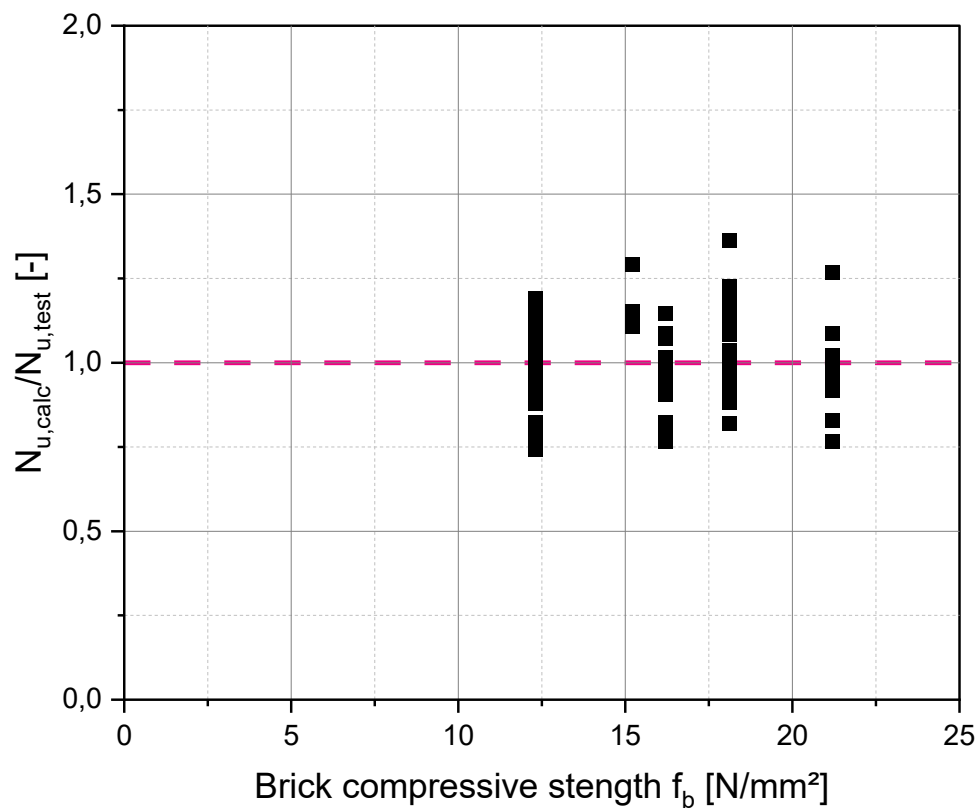


Fig. 9:  $N_{u,calc}/N_{u,test}$  vs. compressive strength [9]

## 5. CONCLUSIONS

Tests with bonded fasteners and undercut anchors under tension loading in solid calcium silicate bricks have been carried out to investigate the influence of embedment depth and compressive strength. In addition, three-point bending tests with specimen cut from bricks have been carried out to evaluate the influence of the base material properties because it was assumed that the results of three-point bending tests give relevant indications on the exponent to be applied on the embedment depth within the calculation of the brick breakout resistance.

It was shown that the increase of the failure loads for the three-point bending tests can be evaluated with an exponent of 1.5 set on the height of the tested beam. This indication was used to investigate the influence of the embedment depth on the failure loads achieved in tension tests with bonded anchors and undercut anchors failing by brick breakout. Finally, it could be shown that the influence of the embedment depth can be described with an exponent of 1.5 ( $h_{ef}^{1.5}$ ).

Different compressive strengths of solid calcium bricks have been investigated. The results show that the increase of the failure loads over a range of compressive strength classes 12 – 20 N/mm<sup>2</sup> can be described with an exponent of 0.3 ( $f_b^{0.3}$ ).

Since several questions are not yet solved, future research work is needed. Further tests with group anchorages should be carried out to estimate the critical axial distance ( $s_{cr}$ ). Also tests with smaller brick dimensions should be carried out to determine the influence of brick dimension and thus also the critical distance to the edge ( $c_{cr}$ ).

## REFERENCES

- [1] MEYER, A.: *Zum Tragverhalten von Injektionsdübel in Mauerwerk* Dissertation, Institute of Construction Materials, University of Stuttgart, Stuttgart, 2005
- [2] WELZ, G.: *Tragverhalten und Bemessung von Injektionsdübel unter Quer- und Schrägzugbelastung im Mauerwerk* Dissertation, Institute of Construction Materials, University of Stuttgart, Stuttgart, 2011
- [3] STIPETIC, M.: *Zum Tragverhalten von Injektionsdübeln in ungerissenem und gerissenem Mauerwerk* Dissertation, Institute of Construction Materials, University of Stuttgart, Stuttgart, 2017

- [4] ETAG 020: *Plastic Anchors for multiple use in Concrete and Masonry for non-structural Applications* European Organisation for Technical Approvals, Brussels, 2006
- [5] EAD 3300076-01-0604: *Metal Injection Anchors for use in Masonry* European Organisation for Technical Approvals, Brussels, 2023
- [6] TR054: *Design Methods for Anchorages with Metal Injection Anchors and Screw Anchors for use in Masonry* European Organisation for Technical Approvals, Brussels, 2022
- [7] TR029: *Design of Bonded Anchors* European Organisation for Technical Approvals, Brussels, 2010
- [8] DIN EN 772-1: *Prüfverfahren für Mauersteine – Teil 1: Bestimmung der Druckfestigkeit* Deutsches Institut für Normung e.V., Berlin, 2016
- [9] PANZEHIR, M.: *Load-Bearing Behaviour and Design of Bonded Anchors in Masonry made of Solid Calcium Silicate Brick* Unpublished dissertation, Institute of Construction Materials, University of Stuttgart, Stuttgart, 2024
- [10] DIN EN 772-6: *Prüfverfahren für Mauersteine – Teil 6: Bestimmung der Biegezugfestigkeit von Mauersteinen aus Beton* Deutsches Institut für Normung e.V., Berlin, 2001
- [11] BUNDESVERBAND KALKSANDSTEININDUSTRIE E.V.: *Kalksandstein – Planungshandbuch: Planung, Konstruktion, Ausführung* Bau+Technik GmbH, Düsseldorf, 2018